PROTEINS: Structure, Function, and Genetics 8:226–236 (1990)

Bundles of Amphipathic Transmembrane α-Helices as a Structural Motif for Ion-Conducting Channel Proteins: Studies on Sodium Channels and Acetylcholine Receptors

Shigetoshi Oiki,[1] Vincent Madison,[2] and Mauricio Montal[3]

[1]Department of Neurosciences, Roche Institute of Molecular Biology, Nutley, New Jersey 07110, [2]Roche Research Center, Hoffmann-La Roche Inc., Nutley, New Jersey 07110, and [3]Departments of Biology and Physics, University of California, San Diego, La Jolla, California 92093-0319.

ABSTRACT **Channel proteins are transmembrane symmetric (or pseudosymmetric) oligomers organized around a central ionic pore. We present here a molecular model of the pore forming structures of two channel proteins with different primary structures and oligomeric size: the voltage-sensitive sodium channel and the nicotinic cholinergic receptor. We report low-energy arrangements of α-helical bundles calculated by semiempiricial potential energy functions and optimization routines and further refined using molecular dynamics. The ion-conducting pore is considered to be a symmetric or pseudosymmetric homooligomer of 3–5 amphipathic α-helices arranged such that the polar residues line a central hydrophilic pathway and the apolar residues face the hydrophobic bilayer interior. The channel lining exposes either charged (Asp, Glu, Arg, Lys) or polar-neutral (Ser, Thr) residues. A bundle of four parallel helices constrained to C_4 symmetry, the helix axis aligned with the symmetry axis, and the helices constrained to idealized dihedral angles, produces a structure with a pore of the size inferred for the sodium channel protein (area ~ 16 Å^2). Similarly, a pentameric array optimized with constraints to maintain C_5 symmetry and backbone torsions characteristic of α-helices adopts a structure that appears well suited to form the lining of the nicotinic cholinergic receptor (pore area ~ 46 Å^2). Thus, bundles of amphipathic α-helices satisfy the structural, energetic, and dynamic requirements to be the molecular structural motif underlying the function of ionic channels.**

Key words: protein structure, ionic pores, neural membranes, protein design, energy minimization, molecular dynamics

INTRODUCTION

Channel proteins are a special class of membrane proteins that mediate the selective passage of ions across the low dielectric constant apolar core of the membrane lipid bilayer (for review see 1). Understanding their mode of action has progressed with the advent of recombinant DNA technology that resulted in the elucidation of the primary structure of several channel proteins.[2–4] A remarkable feature inferred from the amino acid sequences is the high homology conservation among members of this family of proteins. They are composed of homologous subunits or domains which contain several transmembrane segments. Further, segments that could be folded into amphipathic transmembrane α-helices are identifiable in all channel proteins for which sequence information is available.[5–9] This is significant because amphipathic α-helices could form a bundle with one side facing an internal hydrophilic pore and the other facing hydrophobic helices or the membrane core. In addition, image analysis of electron micrographs obtained from ordered arrays of channel proteins in their native membrane environment produced low resolution images (~ 18 Å) that are consistent with radial symmetric or pseudosymmetric protein assemblies organized around a central aqueous pore.[10,11] These key features, homology and symmetry, raise the notion that a unifying motif in the biological design of ion channels is an array of transmembrane α-helices arranged such that amphipathic helices face a central hydrophilic pore whereas hydrophobic helices sur-

Received December 18, 1989; revision accepted March 16, 1990.

Address reprint requests to Mauricio Montal, Departments of Biology and Physics, University of California, San Diego, La Jolla, CA 92093–0319.

S. Oiki's present address is Department of Physiology, Kyoto University Faculty of Medicine, Kyoto 606, Japan.

TABLE I. Amino Acid Sequence of the Synthetic Channel Peptides That Mimic the Pore-Forming Segments of the Sodium Channel (Sc1) and the Nicotinic Acetylcholine Receptor (M2δ)

	1	5	10	15	20
Sc1:	Asp-Pro-Trp-Asn-	Trp-Leu-Asp-Phe-Thr	Val-Ile-Thr-Phe-Ala-	Tyr-Val-Thr-Glu-Phe-	Val-Asp-Leu
	1	5	10	15	20
M2δ:	Glu-Lys-Met-Ser-	Thr-Ala-Ile-Ser-Val-	Leu-Leu-Ala-Gln-Ala-	Val-Phe-Leu-Leu-Leu-	Thr-Ser-Gln-Arg

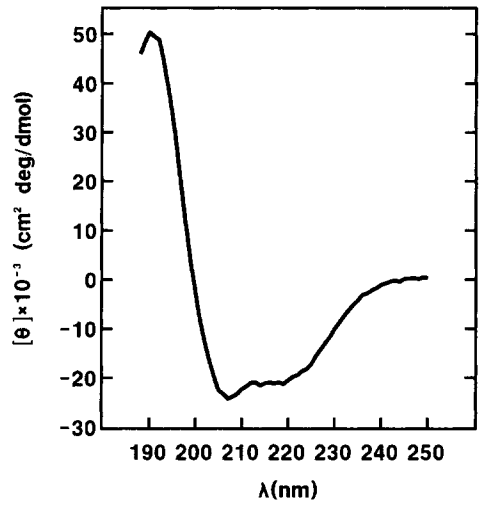

Fig. 1. CD spectrum of AChR M2δ peptide in trifluoroethanol. The peptide concentration was 78 μM and the temperature 20°C.

round this inner bundle as an interface with the hydrophobic environment of a lipid bilayer.[12–18] Such structure accounts for the geometric and symmetry constraints of channel proteins, provides a rationale for the extensive homology, and accounts for the diversity of channel proteins in so far as this would be determined by the sequence specificity and oligomer size.

Here, we examine the energetic feasibility of this functional unit (inner bundle which lines the pore) as a minimal motif from the analysis of two distinct channel proteins that have different primary structures and oligomeric size: the voltage-sensitive sodium channel from mammalian brain that exhibits 4-fold symmetry (for review see 19) and the nicotinic cholinergic receptor from electric fishes that has 5-fold symmetry (for review see 20). This analysis is based on our studies of synthetic peptide channels designed to mimic the pore forming segments of both the voltage-dependent sodium channel[15–17] and the nicotinic acetylcholine receptor.[15,18] A peptide with identical sequence to one of the pore segments was incorporated into planar lipid bilayers where it self-assembled into a homooligomer. The ion-conduction characteristics of the synthetic channel peptides emulate the properties of the ion-conductive pathway of their respective authentic channel proteins and, therefore, provide relevant model systems to pursue questions about the structure of channel proteins. We report the low-energy arrangements of α-helical bundles of homooligomers calculated by semiempirical potential energy functions and optimization routines and further refined using molecular dynamics and reminimization.[21] We conclude that a motif consisting of a bundle of amphipathic α-helices satisfies the structural, energetic, and dynamic requirements for biological function of ionic channels; a preliminary account of this research was presented elsewhere.[17,18]

METHODS

Structure of the Peptides

The sequences of the peptides (Table I) correspond to those designated as the third transmembrane segment of repeat I from rat brain sodium channel I (Sc1)[8,16,17,22–25] and the M2 segment of the delta subunit from the *Torpedo californica* acetylcholine receptor (AChR) channel (M2δ),[18,26–28] respectively. Empirical secondary structure predictors suggest that these sequences could form amphipathic α-helices.[29–32]

Circular Dichroism (CD) Spectroscopy

CD indicates that both peptides adopt helical conformations in trifluoroethanol (99+% pure from Aldrich). As shown in Figure 1, the AChR M2δ peptide exhibits the characteristic double minima at ~222 nm and ~208 nm with a prominant peak at ~190 nm. Spectra were fitted as described.[3] Calculated parameters of the fitted curves expressed as percentage α, β, turn, or random were α = 57%; β = 0, turn = 0, and random chain = 43%. Corresponding values for the Sc1 peptide were α = 30%, β = 35%, turn = 5%, and random chain = 30%. CD spectra were recorded on a Cary 60 recording spectropolarimeter in a 0.2 mm pathlength cell at a peptide concentration of 78 μM. Temperature was 20°C.

Computation

Peptide structures were built and adjusted using the Roche Interactive Molecular Graphics (RIMG) package.[34] The CHARMM program system[21] (version 19) was used for constrained energy minimization and molecular dynamics optimization of the structures with modified version 18 parameters.[35] As appropriate for the various calculations, constraints were used for symmetry and to maintain regular helical backbone dihedral angles of $\phi = -45$ and $\psi = -60$ with a force constant of 200 kcal/mol per radian (1 kcal = 4.18 kJ). For pairwise electro-

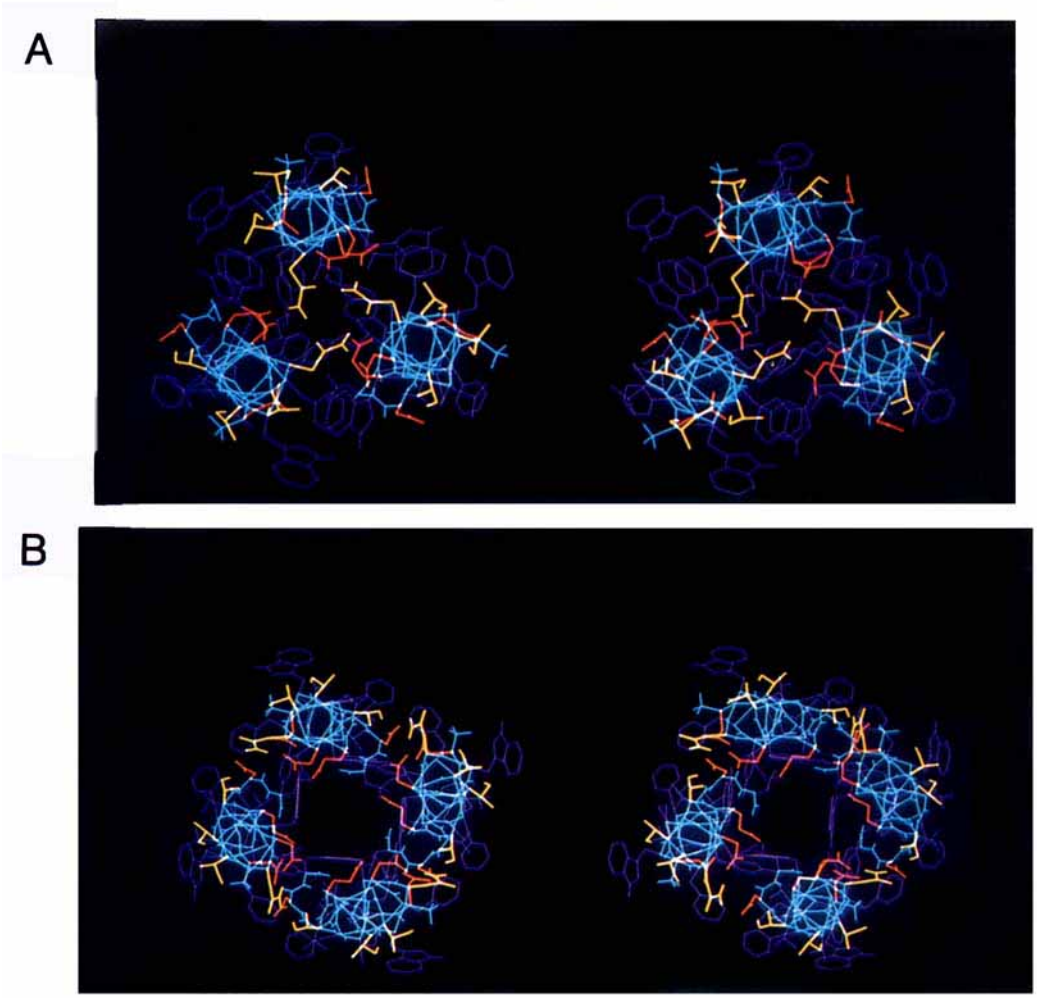

Fig. 2. Stereo, end-view of energy optimized parallel trimer **(A)** and tetramer **(B)** of the sodium channel Sc1 segment. Color code: light blue—α-carbon backbone; red—acidic; blue—basic; yellow-polar-neutral; and purple—lipophilic residues. The N-terminus is in the front and is assigned to the intracellular face of the membrane.[8,45]

static energies, the dielectric constant was *r*, the distance between the charges. Throughout, minimization was conducted using 200 steepest descent steps followed by assumed-basis Newton–Raphson steps until the energy converged to 0.01 kcal/mole (up to 5000 steps). The energy of a peptide array was optimized in four steps: minimization, 15 ps dynamics at 300 K, 9 ps dynamics while gradually cooling to near 0 K, and reminimization.

Sodium Channel

Atomic coordinates of the helical backbone from hemerythrin[36] and zervamycin[37] were utilized as templates for helical structures.[36,37] An array of three or four parallel helices was symmetrically placed about an axis through the center of the array parallel to the helices. The polar residues (especially the acidic side chains) were placed at the interior of the assembly and the apolar residues (especially the aromatic side chains) at the exterior surface of each helix. This is the initial structure (see Table II). The three structures considered, with the symmetry used in parentheses, were as follows: a parallel trimer (C_3), a parallel tetramer (C_4), and an antiparallel tetramer (D_2).

Ion-pore interactions were explored by placing four sodium ions at regular intervals inside the pore formed by the parallel tetramer. The ions were constrained to the axis of the pore.

Acetylcholine Receptor Channel

The 23-mer M2δ-like peptide was placed in a pentameric, C_5-symmetric, parallel array using the previous tetrameric sodium channel model as a template for an individual helix (Table II). Peptide side chains were adjusted by means of interactive molecular graphics to avoid short steric contacts. The pentameric array was then optimized using energy minimization and molecular dynamics with constraints to maintain C_5 symmetry. Four initial orientations

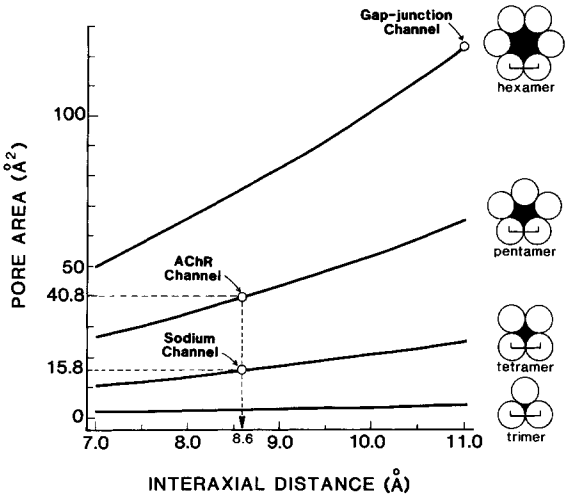

Fig. 3. Geometric relationship between oligomeric bundles and pore area. Pore area is calculated geometrically as a function of interaxial distance in the range from 7 to 11 Å, which are crystallographically observed values, and the helix diameter is assumed to be equal to the interaxial distance. Electrophysiologically determined pore areas at narrowest extents are 15.8 Å^2 and 40.8 Å^2 for Na channel and AChR channel, respectively.[1] These areas are obtained if the interaxial distance is 8.6 Å. A tightly packed hexamer should have, therefore, a pore area of 76 Å^2, a value in accord with modeling,[57] but in contrast to reported values for a biological hexameric channel, the gap junction. Gap-junctional channel pore area is an estimate.[58]

differing by successive rotations of 100° about the axis of an individual helix were tested. Subsequently, four additional orientations were obtained from the lowest energy structure of the first set by rotating each helix ± 100° or ± 200° about its axis.

Three $Tris^+$ cations were placed at regular intervals inside the pore formed by the parallel pentamer. Energy optimization was done without symmetry constraints.

RESULTS AND DISCUSSION

Sodium Channel

The 22-mer Sc1-like peptide is amphipathic

Optimized helical structures of Sc1 in a trimer and a tetramer are shown in Figure 2. Although individual helices in either trimer or tetramer have similar structure, we focus on the helices in the tetramer. The arrays have regular, aligned α-helices except for the C-terminus. Orthographic projections indicate the segregation of hydrophilic and lipophilic residues on opposite faces of the helical cylinder. The two charged acidic residues Asp-7 and Glu-18 are aligned. The length of the helix is 32 Å, sufficient to traverse the hydrocarbon core of the membrane.[39]

The monomeric peptide would have high energy within the hydrophobic interior of the lipid bilayer due to its low mean hydrophobicity (0.44). However, an oligomeric array of amphipathic helices meeting with their polar surfaces facing inward could form a putative ion-conductive path through the assembly. The hydrophobic moment[40] calculated for the optimized structure is 0.19, a feature that is consistent with an oligomeric structure of the peptide in the membrane.

TABLE II. Symmetry and Inter-Helical Orientation for Optimized Oligomeric Arrays

Structure	Symmetry	Orientation angle between helical axes
Sodium channel		
Parallel trimer	C_3	5
Parallel tetramer	C_4	15
Antiparallel tetramer	D_2	175
Acetylcholine channel		
Parallel pentamer	C_5	10

Qualitatively the characteristic features of this Sc1 segment would also prevail for the other Sc segments because of their highly homologous sequences.[17] Therefore, a homooligomer of Sc1 is a plausible model for the heterooligomer in the channel protein.

Structure of the channel is oligomeric—parallel tetramer

Figure 2A shows an orthographic projection through a trimer of helices with C_3 symmetry. The helices are parallel and aligned. The structure displays the nonpolar side chains along the exterior surface and the polar residues at the interior of the assembly. The dot surface view of the model indicates that the trimer is a close-packed occluded structure, without a patent polar pore. The interior of the array is stabilized by strong helix–helix interactions and by polar interactions between residues facing the lumen of the cluster, such as the polar threonine residues (Thr-9, Thr-12). Evidently, the trimeric array cannot account for the known permeability characteristics of the authentic sodium channel protein or the peptide assembly since the largest cross-sectional area is calculated to be 4.9 Å^2 (Fig. 3) while electrophysiological studies established an effective cross-sectional area for the permeability path of the sodium channel of 16 Å^2 (for review see 1). It follows, then, that the minimum array capable of accounting for the observables in both the authentic sodium channel and the synthetic Sc1 channel is a bundle of four packed α-helices (see Fig. 3). Note that assuming the helix is a rigid cylinder of 9 Å diameter[40–43] the geometrically calculated area of a pore produced by a tetramer of helices is 16 Å^2, as illustrated in Figure 3. This value is consistent with both the 4-fold symmetry of the sodium channel[3,8] and the dimensions of its selectivity filter (cf. 1). By contrast, in the antiparallel tetrameric array optimized with D_2 symme-

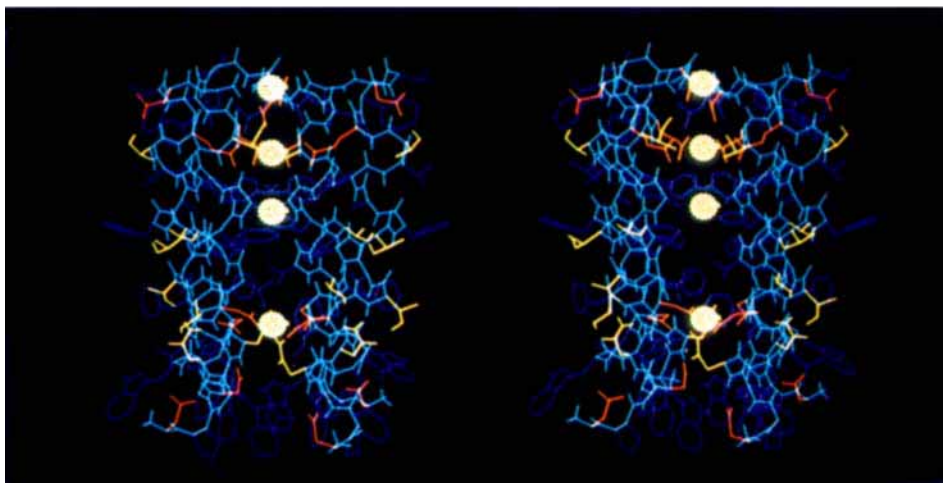

Fig. 4. Stereo, side-view of the parallel tetramer of Sc1 with four Na^+ ions. These four Na^+ ions were placed at regular intervals for the initial structure. The optimized structure represents ion-helix interaction. The uneven distribution of Na^+ ions indicates positions of local energy minima on the axis of the pore. The N-terminus is at the bottom of the structure.

try, kinking of the C-terminus occludes the pore so that it has a patent cavity, but without an access path to the exterior of the pore. We focus, therefore, on the parallel tetramer because it appears to be a structure well suited to form the lining of the ionic pore of the sodium channel protein.[3,8,17]

Figure 2B, shows a stereo end-view of the parallel tetramer (C_4). Optimization with the parallel bundle constrained to C_4 symmetry and the helices constrained to idealized dihedral angles, produced a structure with a pore of the size inferred for the sodium channel protein (Fig. 3).

Figure 4, shows the corresponding side view of the parallel tetrameric array. The N-terminus is at the bottom of the assembly and is assigned to the intracellular side of the membrane[8,45] assuming that the connecting loop between Sc and Sd segments does not traverse the membrane.[8]

We focus now on detailed features of the pore formed by the C_4-symmetric tetramer. The bundle shows a left-handed twist with an interhelical angle of 15° (see Fig. 4, and Table II), which is considered the most stable arrangement.[42] Note that the optimized structures maintain the segregation of polar and nonpolar residues of the original model. At the N-terminus of the assembly, the indole ring of the tryptophanes (Trp-3) hydrogen-bond with aspartate (Asp-1) and form a square vestibule at the entry of the pore. This structure may provide a rigidity of the entrance, while the dipole moment of the indole rings, which points almost parallel to the pore axis, may facilitate passage of ions. Note that the pore is lined by two clusters of acidic residues (Asp-7s and Glu-18s), although their mutual electrostatic repulsion forces them away from the center of the pore.

We turn now to outline a putative pathway of Na^+ ions as they traverse the pore lined by the parallel bundle of four amphipathic α-helices. Figure 4 shows the side view of the C_4 array containing four Na^+ ions. The position of these three sodium ions on the pore axis, except for C-terminal one, could coincide to the three energy wells in the four barrier, three well Eyring rate theory model, calculated from electrophysiological analysis of sodium channel proteins.[46–48] The fourth Na^+ ion at the C-terminus is artificial because there is a free carboxyl group in this position in the model peptide, but not in channel proteins.

We proceed to describe imaginary transverse sections taken across the bundle and progressing from the N-terminus to the middle and then, to the C-terminus (Fig. 5A,B,C). The three planes are illustrated with Na^+ ions showing the van der Waals envelope (dotted surface) that indicate the sum of the sodium ion and oxygen radii. Na^+ enters the pore through the vestibule provided by the four tryptophan side chains. The position of the first Na^+ is bounded by a cross section of 2 × 2 Å. The negatively charged side chains of the first ring of aspartates (Asp-7) solvate the incoming Na^+. Na^+ ions proceed to the middle of the pore where they are surrounded by apolar residues. The second Na^+ is solvated by the phenolic hydroxyl groups of Tyr-15 at a region with dimensions of 4 × 4 Å. The second ring of negatively charged residues, Glu-18, interacts with the Na^+ and promotes its transfer towards the exit path from the pore. The third Na^+ interacts with Glu-18 carboxylate groups and the fourth Na^+ is between Phe-19 and the C-terminus. In both locations the pore dimensions are 3 × 3 Å. Throughout this trajectory, the effective pore area is ≥ 16 $Å^2$ the size at its narrowest point, located at residue

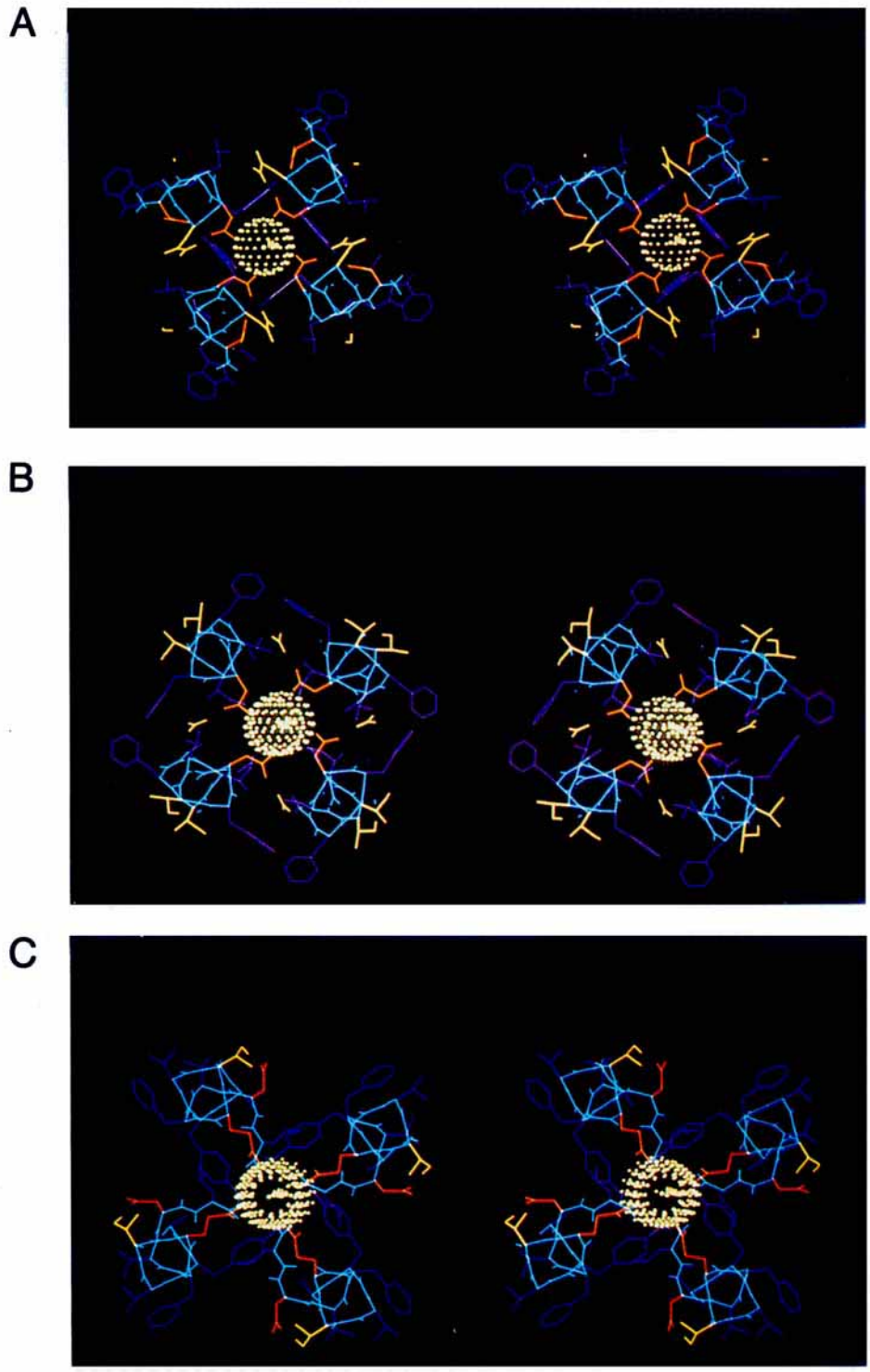

Fig. 5. Cross sections of the parallel tetramer at the level of the N-terminus **(A)**, the middle of the pore **(B)**, and the C-terminus **(C)**. The dot surface radius of the Na^+ ion represents the sum of the Na^+ ion radius and the oxygen radius (total 2.8 Å).

Tyr-15. Thus, the C_4 symmetric bundle appears to account for the geometric constraints of the sodium channel.

The selectivity filter of the sodium channel has been phenomenologically described as a narrow region within the pore pathway that contains acidic

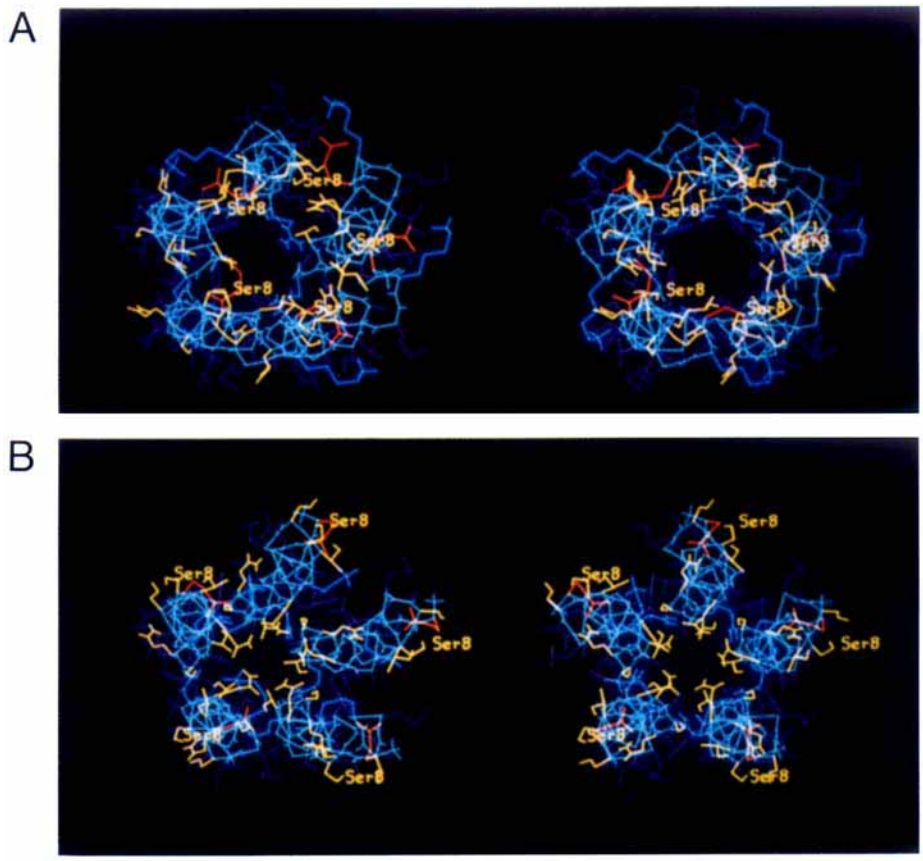

Fig. 6. Stereo, end-view of the optimized parallel pentamer of the acetylcholine receptor M2δ segment, with Ser-8 inside **(A)** and outside **(B)** the lumen of the pore. The N-terminus is in the front and is assigned to the intracellular face of the membrane.[3]

groups (cf. 1,49). It is known that the conductance of sodium channels diminishes as the pH of the electrolyte bathing the membrane is reduced. The pH at which the conductance is reduced by 50% is 5.2 when titrated from the cell exterior and 5.8 from the interior. It is worthy of note that these values closely reflect the relative apparent pK_as of aspartate (4.0) and glutamate (4.2) and that the electrical distances of H^+ binding sites are 20–25% from the pore exterior and 25% from the interior, which closely match the positions of Glu-18 and Asp-7. This fact lends credence to the assigned transmembrane loci of Asp-7 and Glu-18 in the C_4 symmetric bundle.

Comparing the empty structures with the Na^+-loaded pore (Figs. 2B and 5) indicates that polar residues move in to solvate the ions and that the individual helices rotate 30° about their axis in the clockwise direction at the levels of Asp-7 and Glu-18, while the square vestibule is preserved.

Acetylcholine Receptor

The 23-mer M2δ-like peptide is amphipathic

End views in Figure 6 of M2δ helices indicate the occurrence of hydrophobic and hydrophilic residues on opposite faces of the helical cylinder. The hydrophobic moment[40] is 0.25. Ser-8, which corresponds to serine 262 in the actual protein sequence, is positioned on the hydrophilic surface. Ser-262 is a reactive site for non-competitive channel blockers[50,51] and is, therefore, presumably exposed to the lumen of the pore.

Structure of the pentameric channel

The 23-mer peptide that mimics the AChR M2δ segment forms channels in lipid bilayers with properties remarkably similar to those of the authentic *Torpedo* AChR,[18] a pentameric complex of five homologous subunits ($\alpha_2\beta\gamma\delta$). Of eight structures with different initial geometries (see Methods), two were calculated to be at least 10% more stable than the other six whose energy was about −200 kcal/mol-peptide chain. These are illustrated in Figure 6A and B. The low-energy structure shown in B was not considered further because Ser-8 faces the exterior of the bundle (contrary to affinity labeling experiments) and the pore diameter is ≤ 2 Å at its narrowest extent (Gln-13). The lowest energy structure shown in A was selected as a plausible model for the

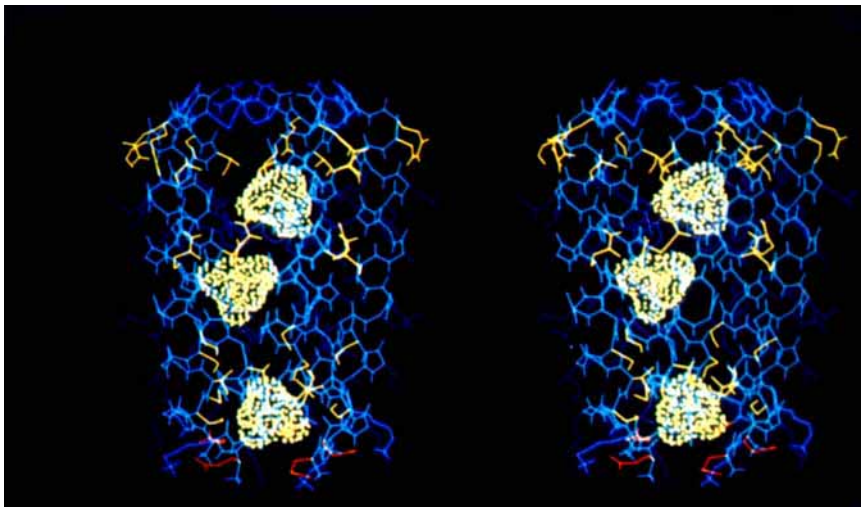

Fig. 7. Stereo, side-view of the M2δ pentamer with three $Tris^+$ ions. The N-terminus is at the bottom of the structure.

AChR pore structure because Ser-8 is exposed on the channel lumen (in accord with chemical labeling) and the bundle has a pore area of ~ 44 Å^2, consistent with the apparent cross section of the authentic protein

The optimized parallel pentamer has a right handed inter-helical twist with orientation angle of 10°. A side view (Fig. 7) shows a funnel shape narrowing at the N-terminus which is thought to be positioned intracellularly (cf. 3). Several leucine residues are sticking out from the outer surface of the pentamer which may interact with neighboring hydrophobic helices in the protein.

We turn now to describe $Tris^+$ ions in the channel. $Tris^+$ is a permeant cation through both the authentic AChR protein and the synthetic M2δ channel peptide. The molecular dimensions of $Tris^+$, as estimated form Corey–Pauling–Koltun models,[52] are 6.0 × 6.9 × 7.7 Å. Three $Tris^+$ cations were placed inside the pentameric array at positions in the vicinity of the N-terminus, the middle, and the C-terminus of the bundle. Energy optimization was conducted on this structure. A side view of the structure displaying the van der Waals envelope of the cations is illustrated in Figure 7 and end-views perpendicular to the axis of the pore lumen are shown in Figure 8. It is evident that the width of the pathway is sufficient to accommodate $Tris^+$ throughout the entire structure, from the entry into the pore to the exit out of it; no steric blockage is discernible. We proceed now to outline a putative pathway of the $Tris^+$ ions as they pass through the lumen of the pore. Figure 8 shows cross sections across the bundle progressing from the N-terminus (A), to the middle (B) and then to the C-terminus (C). At the N-terminus, Glu-1 bridges the amino groups of the N-terminus and Lys-2 of each helix. This generates a ring of charged residues facing the putative intracellular end of the pore structure. Glu-1 and Lys-2 are highly conserved residues. This fact is significant since the minimized model considers five identical M2δ helices and, at this end of the pore structure, the corresponding $\alpha_2\beta\gamma\delta$ pentamer would be virtually identical. At this location, the dimensions of the pore are 6 × 6 Å (width × height, Å). The position of the first $Tris^+$ is bounded by an area of 5 × 6 Å which is then followed by a relative narrowing of the pore at the location of Ser-8; the dimensions are 4 × 4 Å. The second $Tris^+$ is located between Ser-8 and Ala-12 at one side of a region with dimensions of 10 × 8 Å. At the third $Tris^+$, the van der Waals spheres of the ion and the phenylalanines appear in close contact and the pore dimension is 4 × 5 Å. The exit path of the pore also exhibits a ring of charged residues: the Arg-23 side chains bridge the C-termini of neighboring helices generating a ring at the putative synaptic side of the bundle with diameter of 10 × 10 Å. Thus, the C_5-symmetric bundle conforms to the general features of the packing arrangement postulated for the $\alpha_2\beta\gamma\delta$ pentamer of the authentic cholinergic receptor. The exterior is lipophilic, the interior more hydrophilic, and Ser-8 (corresponding to Ser-262 of the AChR δ subunit) is exposed on the channel lumen.

Recently, AChRs with mutations at various sites in the M2 segment, were expressed in *Xenopus* oocytes after injection of cloned mRNAs and the single channel properties analyzed.[53,54] Focusing on M2δ, a change in Glu-1 (Glu-255) for Gln produced AChRs with a drastic reduction in conductance (≥ 2-fold) and in the sensitivity of outward and inward channel currents to intracellular and extracellular

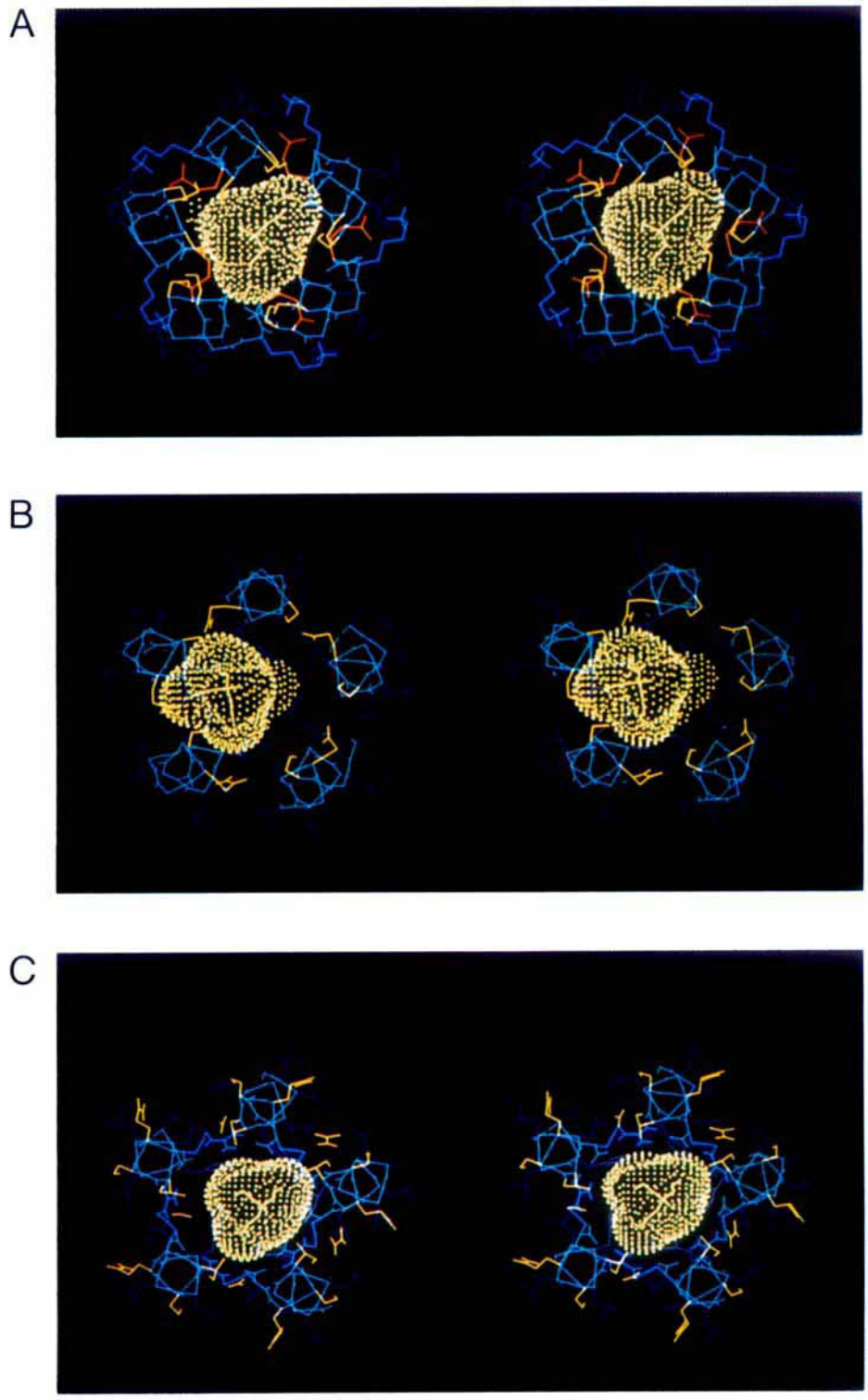

Fig. 8. Cross-sections of the M2δ pentamer—at the level of the N-terminus **(A)**, the middle of the pore **(B)**, and the C-terminus **(C)**. For these cross-sections, the dot surface of the $Tris^+$ ion has been increased by adding the radius of an oxygen atom.

[Mg^{2+}], respectively.[53] This evidence is in accord with the model structure shown in Figure 8, where Glu-1 hydrogen bonds to Lys-2 (the N-terminal amino group would be absent in the protein). A single mutation with a change in Ser-8 corresponding to Ser-262 of M2δ, to alanine reduced the binding affinity of the AChR channel for a local anesthetic analogue of lidocaine (QX-222) as assayed by the channel blocking effect of QX-222.[54,55] The $\alpha_2\beta\gamma\delta$ stoichiometry of AChRs enables the addition or deletion of serine residues at the conserved position corresponding to Ser-8 in the M2δ-mimicking peptide yielding mutant AChRs with 0, 1, 2, 3, or 4 serine residues at this site. The binding affinity of mutant AChRs for the QX-222 channel blocker increased with the number of serine residues exhibiting a change of favorable binding energy amounting to 0.21 kcal/mol QX-222 per serine residue.[54] This result is in gratifying accord with affinity labeling and sequencing results,[50,51] the expectation of residues containing OH as contributors to the structure lining the channel of a water-filled pore (cf. 56), the transmembrane arrangement of M2,[53] and the channel activity of the M2δ mimicking peptide.[18]

In summary, we conclude that a motif consisting of a bundle of amphipathic α-helices satisfies the structural, energetic, and dynamic requirements for the function of biological ionic channels.

ACKNOWLEDGMENTS

We are indebted to William Sun for his participation in the CD measurements and Murray Goodman for the use of his CD facility. This work was supported in part by the NIMH (MH-44638), NIMH (MH 00778, Research Scientist Award), NIGMS (GM-42340), and ONR (N00014-89-J-1469) to M. Montal.

REFERENCES

1. Hille, B. "Ionic Channels of Excitable Membranes." Sinauer Associates, Sunderland, MA: 1984:426.
2. Numa, S., Noda, M. Molecular structure of sodium channels. Ann. N.Y. Acad. Sci. 479:338–355, 1986.
3. Numa, S. A molecular view of neurotransmitter receptors and ionic channels. Harvey Lect. 83:121–165, 1989.
4. Schofield, P.R., Darlison, M.G., Fujita, N., Burt, D.R., Stephenson, F.A., Rodriguez, H., Rhee, L.M., Ramachandran, J., Reale, V., Glencorse, T.A., Seeburg, P.H., Barnard, E.A. Sequence and functional expression of the $GABA_A$ receptor shows a ligand-receptor super-family. Nature (London) 328:221–227, 1987.
5. Finer-Moore, J., Stroud, R.M. Amphipathic analysis and possible formation of the ion-channel in an acetylcholine receptor. Proc. Natl. Acad. Sci. U.S.A. 81:155–159, 1984.
6. Guy, H.R. A structural model of the acetylcholine receptor channel based on partition energy and helix packing calculations. Biophys. J. 45:249–261, 1984.
7. Guy, H.R., Seetharalamu, P. Molecular model of the action potential sodium channel. Proc. Natl. Acad. Sci. U.S.A. 83:508–512, 1986.
8. Greenblatt, R.E., Blatt, Y., Montal, M. The structure of the voltage sensitive sodium channel inferences derived from computer-aided analysis of the *Electrophorus electricus* primary structure. FEBS Lett. 193:125–134, 1985.
9. Greeningloh, G., Rienitz, A., Schmitt, B., Methfessel, C., Zensen, M., Beyreuther, K., Gundelfinger, E.D., Betz, H. The strychnine-binding subunit of the glycine receptor shows homology with nicotinic acetylcholine receptors. Nature (London) 328:215–220, 1987.
10. Toyoshima, C., Unwin, N. Ion channel of acetylcholine receptor reconstructed form images of postsynaptic membranes. Nature (London) 336:247–250, 1988.
11. Unwin, N., Toyoshima, C., Kubalek, E. Arrangement of the acetylcholine receptor subunits in the resting and desensitized states, determined by cryoelectron microscopy of crystallized *Torpedo* postsynaptic membranes. J. Cell Biol. 107:1123–1138, 1988.
12. Mueller, P., Rudin, D.O. Action potentials induced in bimolecular lipid membranes. Nature (London) 217: 713–719, 1968.
13. Fox, R.O., Jr., Richards, F.M. A voltage-gated ion channel model inferred from the crystal structure of alamethicin at 1.5-Å resolution. Nature (London) 300:325–330, 1982.
14. Furois-Corbin, S., Pullman A. A possible model for the inner wall of the acetylcholine receptor channel. Biochim. Biophys. Acta 984:339–350, 1989.
15. Montal, M., Oiki, S., Danho, W. Channel protein engineering: A novel strategy to establish structure-function correlations in the voltage-dependent sodium channel. Biophys. J. 53:35a, 1988.
16. Oiki, S., Danho, W., Montal, M. Synthesis of an ion-channel forming peptide predicted from the primary structure of the voltage sensitive sodium channel. Soc. Neurosci. 13:576 Abstr. 163.2, 1987.
17. Oiki, S., Danho, W., Montal, M. Channel Protein Engineering: Synthetic 22-mer peptide from the primary structure of the voltage-sensitive sodium channel forms ionic channels in lipid bilayers. Proc. Natl. Acad. Sci. U.S.A. 85:2393–2397, 1988.
18. Oiki, S., Danho, W., Madison, V., Montal, M. M2δ, a candidate for the structure lining the ionic channel of the nicotinic cholinergic receptor. Proc. Natl. Acad. Sci. U.S.A. 85:8703–8707, 1988.
19. Jan, L.Y., Jan, Y.N. Voltage-sensitive ion channels. Cell 56:13–25, 1989.
20. Changeux, J.P., Revah, F. The acetylcholine receptor molecule: Allosteric sites and the ion channel. Trends Neurosci. 10:245–250, 1987.
21. Brooks, B.R., Bruccoleri, R.E. Olafson, B.D., States, D.J., Swaminathan, S., Karplus, M. CHARMM: A program for macromolecular energy, minimization and dynamics calculations. J. Comp. Chem. 4:187–217, 1983.
22. Noda, M., Shimizu, S., Tanabe, T., Takai, T,. Kayano, T., Ikeda, T., Takahashi, H., Nakayama, H., Kanaoka, Y., Minamino, N., Kangawa, K., Matsuo, M.H., Raftery, M.A., Hirose, T., Inayama, S., Hayashida, H., Miyata, T., Numa, S. Primary structure of *Electrophorus electricus* sodium channel deduced from cDNA sequence. Nature (London) 312:121–127, 1984.
23. Noda, M., Ikeda, T., Kayano, T., Suzuki, H.,, Takashima, H., Kurasaki, M., Takahashi, H., Numa, S. Existence of distinct sodium channel messenger RNAs in rat brain. Nature (London) 320:188–192, 1986.
24. Kayano, T., Noda, M., Flockerzi, V., Takahashi, H., Numa, S. Primary structure of rat brain sodium channel III deduced from the cDNA sequence. FEBS Lett. 228:187–194, 1988.
25. Auld, V.J., Goldin, A.L., Krafte, D.S., Marshall, J., Dunn, J.M., Catterall, W.A., Lester, H.A., Davidson, N., Dunn, R.J. A rat brain Na^+ channel α subunit with novel gating properties. Neuron 1:449–461, 1988.
26. Noda, M., Takahashi, H., Tanabe, T., Toyosato, M., Furutami, Y. Hirose, T., Asai, M., Inayama, S., Miyata, T., Numa, S. Primary structure of the α-subunit precursor of *Torpedo californica* acetylcholine receptor deduced from cDNA sequence. Nature (London) 299:793–797, 1982.
27. Noda, M., Takahashi, H., Tanabe, T., Toyosato, M., Kikotani, S., Hirose, T., Asai, M., Takashima, H., Inayama, S., Miyata, T., Numa, S. Primary structures of β- and δ-subunit precursor of *Torpedo californica* acetylcholine receptor deduced from cDNA sequences. Nature (London) 301: 251–255, 1983.
28. Noda, M., Takahashi, H., Tanabe, T., Toyosato, M., Kikotani, S., Furutami, Y., Hirose, T., Takashima, H., Inayama, S., Miyata, T., Numa, S. Structural homology of

Torpedo californica acetylcholine receptor subunits. Nature (London) 302:528–532, 1983.
29. Chou, P.Y., Fasman, G.D. Prediction of the secondary structure of proteins from their amino acid sequence. Adv. Enzymol. 47:45–148, 1978.
30. Garnier, J., Osguthorpe, D.J., Robson, B. Analysis of the accuracy and implications of simple methods for predicting the secondary structure of globular proteins. J. Mol. Biol. 120:97–120, 1978.
31. Robson, B., Garnier, J. "Introduction to Proteins and Protein Engineering." Amsterdam: Elsevier, 1986, 699.
32. Schiffer, M,. Edmunson, A.B. Use of helical wheels to represent the structures of proteins and to identify segments with helical potential. Biophys. J. 7:121–135, 1967.
33. Hennessey, J.P. Jr., Johnson, W.C. Jr. Information content in the circular dichroism of proteins. Biochemistry 20: 1085–1094, 1981.
34. Mueller, K., Ammann, H.J., Doran, D.M., Gerber, P., Schrepfer, G. Aspects and applications of computer-assisted molecular modeling to drug design (CAMMDD). In: "Innovative Approaches in Drug Research" (A.F. Harms, ed.). Amsterdam: Elsevier, 1986:125–139.
35. Madison, V., Berkovitch-Yellin, Z., Fry, D., Greeley, D., Toome, V. Conformations of three peptides deduced from experiments and molecular energetics In: "Synthetic Peptides. Approaches to Biological Problems" (J.P. Tam and E.T. Kaiser, eds.). New York: Liss, 1989: 109–123.
36. Smith, J.L., Hendrickson, W.A. Structure of trimeric haemerythrin. Nature (London) 303:86–88, 1983.
37. Karle, I.L., Sukumar, M., Balaram, P. Parallel packing of alpha-helices in crystals of the zervamicin IIA analog Boc-Trp-Ile-Ala-Aib-Leu-Aib-Pro-OMe.2$H_2$0. Proc. Natl. Acad. Sci. U.S.A. 83:9284–9288, 1986.
38. Weber, P.C., Salemme, F.R. Structural and functional diversity in 4-α-helical proteins. Nature (London) 287:82–84, 1980.
39. Blaurock, A.E., Wilkins, M.H.F. Structure of frog photoreceptor membranes. Nature (London) 223:906–909, 1969.
40. Eisenberg, D., Schwarz, E., Komaromy, M., Wall, R. Analysis of membrane and surface protein sequences with the hydrophobic moment plot. J. Mol. Biol. 179:125–143, 1984.
41. Chothia, C., Levitt, M., Richardson, D. Helix to helix packing in proteins. J. Mol. Biol. 145:215–250, 1981.
42. Chou, K.-C., Maggiora, G.M., Nemethy, G., Scheraga, H.A. Energetics of the structure of the four-alpha-helix bundle in proteins. Proc. Natl. Acad. Sci. U.S.A. 85:4295–4299, 1988.
43. Furois-Corbin, S., Pullman, A. Theoretical study of the packing of α-helices into possible transmembrane bundles. Sequences including alanines, leucines and serines. Biochim. Biophys. Acta 902:31–45, 1987.
44. Furois-Corbin, S., Pullman, A. Theoretical study of the packing of α-helices of poly(L-alanine) into transmembrane bundles. Possible significance for ion transfer. Biochim. Biophys. Acta 860:165–177, 1986.
45. Stuhmer, W., Conti, F., Suzuki, H., Wang, X., Noda, M., Yahagi, N., Kubo, H., Numa, S. Structural parts involved in activation and inactivation of the sodium channel. Nature (London) 339:597–603, 1989.
46. Hille, B. Ionic selectivity, saturation, and block in sodium channels: A four-barrier model. J. Gen. Physiol. 66:535–560, 1975.
47. Yamamoto, D., Yeh, J.Z., Narahashi, T. Voltage-dependent calcium block of normal and tetramethrin-modified single sodium channels. Biophys. J. 45:334–337, 1984.
48. Sheets, M.F., Scanley, B.E., Hanck, D.A., Makielski, J.C., Fozzard, H.A. Open sodium channel properties of single canine cardiac purkinje cells. Biophys. J. 52:13–22, 1987.
49. Begenisich, T. Molecular properties of ion permeation through sodium channels. Annu. Rev. Biophys. Biophys. Chem. 16:247–263, 1987.
50. Giraudat, J., Dennis, M., Heidmann, T., Chang, J.Y., Changeux, J.-P. Structure of the high-affinity binding site for non-competitive blockers of the acetylcholine receptor: Serine-262 of the δ-subunit is labeled by [^{3}H]chlorpromazine. Proc. Natl. Acad. Sci. U.S.A. 83:2719–2723, 1986.
51. Oberthür, W., Hucho, F. Photoaffinity labeling of functional states of the nicotinic acetylcholine receptor. J. Protein Chem. 7:141–150, 1988.
52. Huang, L.Y.M., Catterall, W.A., Ehrenstein, G. Selectivity of cations and nonelectrolytes for acetylcholine-activated channels in cultured muscle cells. J. Gen. Physiol. 71:397–410, 1978.
53. Imoto, K., Busch, C., Sakmann, B., Mishina, M., Konno, T., Nakai, J., Bujo, H., Mori, Y., Fukuda, K., Numa, S. Rings of negatively charged amino acids determine the acetylcholine receptor channel conductance. Nature (London) 335:645–648, 1988.
54. Leonard, R.J., Labarca, C.G., Charnet, P., Davidson, N., Lester, H.A. Evidence that the M2 membrane spanning region lines the ion channel pore of the nicotinic receptor. Science 242:1578–1581, 1988.
55. Neher, E., Steinbach, J.H. Local anesthetics transiently block currents through single acetylcholine receptor channels. J. Physiol. (London) 277:153–176, 1978.
56. Eisenman, G., Dani, J.A. An introduction to molecular architecture and permeability of ionic channels. Annu. Rev. Biophys. Biophys. Chem. 16:205–226, 1987.
57. Lear, J.D., Wasserman, Z.R., DeGrado, W.F. Synthetic amphiphilic peptide models for protein ion channels. Science 240:1177–1181, 1988.
58. Spray, D.C., Bennett, M.V.L. Physiology and pharmacology of gap junctions. Annu. Rev. Physiol. 47:281–303, 1985.